Chem Soc Rev

On Decomposition, Degradation, and Voltammetric Deviation: The Electrochemist's Field Guide to Identifying Precatalyst Transformation

Journal:	*Chemical Society Reviews*
Manuscript ID	CS-SYN-10-2018-000851.R2
Article Type:	Tutorial Review
Date Submitted by the Author:	09-Mar-2019
Complete List of Authors:	Lee, Katherine; University of North Carolina, Chemistry McCarthy, Brian; University of North Carolina, Chemistry Dempsey, Jillian; University of North Carolina, Chemistry

Journal Name

ARTICLE

On Decomposition, Degradation, and Voltammetric Deviation: The Electrochemist's Field Guide to Identifying Precatalyst Transformation

Received 00th January 20xx,
Accepted 00th January 20xx

DOI: 10.1039/x0xx00000x

www.rsc.org/

Katherine J. Lee,[a,†] Brian D. McCarthy[a,†] and Jillian L. Dempsey[a,*]

What is the identity of the true electrocatalytic species? This fundamental question has plagued the molecular electrocatalysis community during its decades-long search for selective and efficient transition-metal based electrocatalysts for fuel forming reactions. Identifying when the added species is a precatalyst that transforms into the active catalyst *in situ* is an extraordinarily complex endeavor. Thankfully, the last decade has witnessed a resurgence of interest in understanding and controlling these transformations, leading to an expansion of the experimental toolkit available to probe catalyst identity. In this Tutorial Review, researchers will learn how the nature of the active catalyst can be uncovered using state-of-the-art electrochemical and spectroscopic methods. Analysis of catalytic voltammograms can quickly furnish qualitative evidence of precatalyst transformation and a library of these tell-tale signs is discussed, along with the chemical phenomena underpinning each feature. Complementary electrochemical and spectroscopic methods for identifying *in situ* generation of heterogeneous catalysts are also presented, outlining the conditions required for correct application with special emphasis on potential pitfalls when studying weakly adsorbed material. Case studies are presented to showcase how these different probes can be integrated to develop a comprehensive picture of precatalyst transformation.

Key Learning Points
1. Successful detection of molecular electrocatalyst transformation or degradation poses unique challenges
2. Visual clues from routine cyclic voltammetry experiments can suggest a molecular species is actually a precatalyst
3. Robust methods are available for detecting and characterizing heterogeneous degradation products
4. Understanding how electrocatalysts decompose or transform can provide important insight for advancing catalyst design
5. In situ methods can be used to confirm the presence of a weakly-adsorbed heterogeneous catalysts

Introduction

The desire to prevent our planet from turning into a post-apocalyptic hellscape has prompted the search for renewable energy-based alternatives to fossil fuels.[1] The electrochemical conversion of energy-poor feedstocks such as H_2O and CO_2 into energy-rich molecules has emerged as one of the most promising pathways for producing fuels from renewable energy sources.[2] However, selectively and efficiently enacting these transformations is nontrivial as they are complex multi-electron, multi-proton processes with high-energy intermediates and multiple possible reaction pathways. These challenges have triggered intense interest in the development of molecular electrocatalysts which have the potential to lower kinetic barriers and improve selectivity.[3–5] Electrocatalysts based on molecular transition metal complexes have garnered considerable attention as their properties and activity can be tuned through intelligent ligand design. One considerable disadvantage of these species is their inherent fragility when exposed to catalytic conditions. Under reducing conditions, the addition of electrons to a metal complex can increase ligand lability or promote ligand saturation (alkylation, carboxylation, hydrogenation, etc.), ultimately leading to demetallation. Meanwhile, the extreme oxidizing potentials required for transformations such as electrochemical H_2O oxidation are also capable of triggering destructive ligand oxidation.[6] In certain cases, the initial molecular complex is actually a precatalyst which changes under electrocatalytic conditions to produce homogeneous or heterogeneous species that are themselves catalytically active.

Identification of the active species is critical for understanding catalysis. The issue of differentiating between catalysis by the species intentionally added to the electrochemical cell and catalysis by a degradation product is

[a] Department of Chemistry, University of North Carolina, Chapel Hill, North Carolina 27599-3290, USA
† These authors contributed equally.
*Corresponding author. Email: dempseyj@email.unc.edu

particularly pressing when working with molecular transition metal complexes because significant resources may be dedicated to evaluating and derivatizing a promising catalytic system.[7] However, the non-ideal case where a purported molecular electrocatalyst is actually a precatalyst is rarely reported and analyzed in detail. This is likely in part due to the less-than-straightforward means of detecting the decomposition or transformation of electrochemically active transition metal complexes into new catalytically active species. The most popular electrochemical methods for evaluating electrocatalysts are non-destructive techniques, such as cyclic voltammetry, and thus only the tiny fraction of the precatalyst at the electrode surface is likely to decompose.[8] In these instances, many standard methods for detecting decomposition which rely on evaluation of the bulk solution are less applicable.[9] Further convoluting the situation is the possibility of weakly adsorbed catalytic material – a topic that has only recently begun to garner serious attention – which can easily elude detection.[10]

Thankfully, a 'renaissance' in rigorous electrochemical methods has paralleled the rise of molecular electrocatalysis research and these techniques greatly improve our ability to identify electrochemical precatalyst transformation.[7,11] In many cases, qualitative assessment of catalytic cyclic voltammograms (CV) can furnish strong preliminary evidence of precatalyst transformation, evidence that can be substantiated with a suite of other electrochemical probes and analytical techniques. In the case of heterogeneous catalyst formation – including heterogeneous materials and heterogenized molecular species – surface characterization techniques can even provide information on the identity of the newly formed active catalyst. This Tutorial Review seeks to highlight these methods and showcase their appropriate application with the goal of improving a researcher's ability to identify precatalyst transformations in their own work and encouraging a healthy degree of skepticism when examining new systems reported in the literature.

Within this review, we define a precatalyst as a molecular species initially dissolved in solution which is not actually an intermediate in the catalytic cycle. Precatalysts can transform into four primary types of active catalysts or catalytic intermediates:

I. ***Molecular, Dissolved****:* A homogeneous molecular species derived from the precatalyst. This type of reactivity has been observed when the species added to solution loses (sometimes irreversibly) a ligand under protic and/or reducing conditions.[12] In other cases, the structural integrity of the molecular remains intact, but the true resting state in the catalytic process is the reduced or oxidized version of the original species added to solution.[13]

II. ***Molecular, Heterogenized (can be adsorbed or suspended)***: A molecular species which can strongly or weakly adsorbed to the electrode and/or precipitate in solution (in effect forming *in situ* a heterogenized molecular active catalyst). An odd duck that has only recently received serious attention is the case of reversible solubility changes during catalysis, wherein catalytic intermediates aggregate in solution – prompting precipitation – and /or adhere to the electrode surface while preserving the integrity of the molecular core.

III. ***Heterogeneous, Dissolved****:* A heterogeneous material in solution, such as suspended nanoparticles.

IV. ***Heterogeneous, Adsorbed****:* A heterogeneous material strongly or weakly adsorbed to the electrode, such as deposited nanoparticles or a film.

Different texts use different nomenclatures to discuss these various transformations. In this text, the phrase ***precatalyst transformation*** will encompass all categories, *except for reversible solubility changes during catalysis* (our odd duck category). Meanwhile, we use the phrase ***degradation*** and ***decomposition*** interchangeably to refer to an irreversible transformation (i.e. ligand loss, demetallation) that generates a new species that is catalytically active. In some cases, transformation of the initial intended molecular catalyst does not result in a catalytically active material – a reaction that is not the main point of this text and (when we do mention it) we delineate as ***deactivation***.

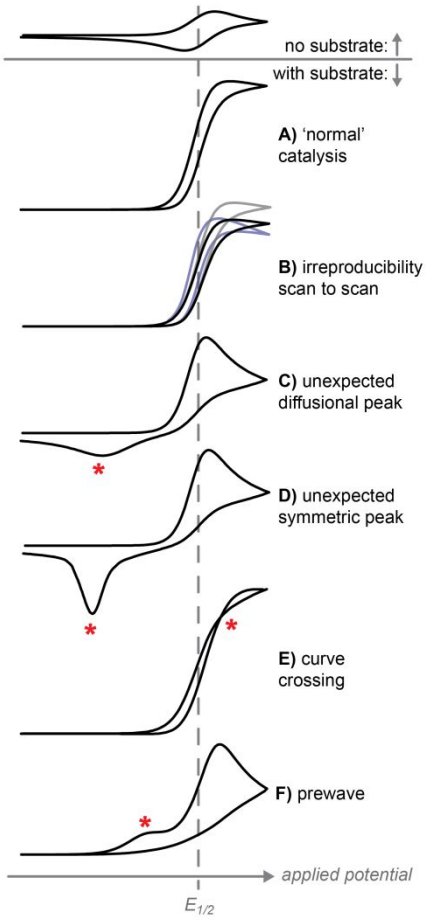

Figure 1. Qualitative signs of catalyst transformation or decomposition as can be observed in cyclic voltammetry

Below, techniques for identifying electrochemically promoted precatalyst transformation are divided into two categories. **Part 1** summarizes voltammetric features that suggest precatalyst transformation to form either homogeneous or heterogeneous catalytically active species. **Part 2** introduces currently available methods for identifying deposition of electroactive species and characterizing electrode-adsorbed catalysts. We then present a series of case studies in **Part 3** to demonstrate how these techniques can be used to detect precatalyst transformation and establish the mechanism of degradation, knowledge which is essential for developing more robust catalysts.

Part 1. Qualitative Signs of Precatalyst Transformation in Cyclic Voltammograms

Cyclic voltammetry is one of the most popular techniques for evaluating molecular electrocatalysts because of the wealth of kinetic and mechanistic information that can be extracted.[8,14,15] In stark contrast, there is little literature discussing the utility of cyclic voltammetry for identifying precatalyst transformation. Often it is deviations from the 'normal' catalytic waveforms that are critical diagnostic tools and thus *it is essential to understand and be able to recognize common catalytic waveforms for molecular homogeneous catalysis*, which we will briefly discuss. For a more thorough discussion of catalytic CVs, the reader is directed to a number of other excellent resources.[8,14,15]

In the absence of substrate – such as protons, H_2O, or CO_2 – a molecular electrocatalyst has its own redox events. Here we focus on the situation where these redox events are both chemically and electrochemically reversible – meaning a 57/(number of electrons) mV peak-to-peak separation of the oxidation and reduction waves.[16] We will not explicitly consider quasireversible redox events, though we expect that many of the techniques discussed here would translate directly. Upon substrate addition, one of these redox events – an oxidation or reduction – can become the trigger for electrocatalysis. Alternatively, the substrate can first interact with the catalyst in a chemical step. In this case, one of the redox events of the substrate-catalyst adduct will trigger electrocatalysis. In the CV, this often manifests as an increase in current at the catalysis-initiating redox couple accompanied by a loss of reversibility of the redox couple, the exception being the total catalysis waveform (see **Case Study 5**).[17–19] However, catalysis is not the only chemical phenomena that can lead to this behavior. After ruling out the possibility that the current increase is just reduction/oxidation of the substrate directly by the electrode,[20] one can qualitatively triage the CV to pinpoint the chemical phenomena underlying the current increase.

Many qualitative signs indicate that reactivity more complex than catalysis alone is taking place. Though the reactivity underlying these signs has been discussed in the literature,[7,9] we have – for the first time – grouped them into one graphic (**Figure 1**). Below, we describe these features and explain how precatalyst transformation can give rise to each case.

Case A ("normal" catalysis)

We put normal in quotation marks here because electrocatalytic waves can assume a variety of shapes depending on experimental parameters (*e.g.*, substrate concentration) and the intrinsic properties of the catalyst (*e.g.*, kinetic parameters). The possible catalytic waveforms for a one-electron, one-substrate reaction were first mathematically described by Savéant and Su.[21] The limiting waveforms were classified into nine zones which are pictorially described in the catalytic kinetic zone diagram (KZD) (**Figure 2**).[15] The 'normal' catalytic wave depicted in **Figure 1** approximates a shape similar to zone K or KS, which is generally observed for 'well-behaved' molecular catalysts. In some cases, the response can be varied across the KZD through careful tuning of experimental parameters (*i.e.*, homogeneous electron transfer rate constant, scan rate, and the initial concentrations of catalyst and substrate) while in others it may be difficult or impossible to reach certain zones due to competing side phenomena such as substrate consumption, catalyst deactivation, product inhibition.[14]

Recently, it has been recognized that the traditional zones are not necessarily directly translatable to more complex, multi-electron catalytic systems. Experimental work extending the KZD to catalytic hydrogen evolution by a cobaloxime catalyst found that, though qualitative parallels exist for each of the classic zones, some deviations in waveforms arise due to electrochemically active reaction intermediates and multiple elementary step rate constants.[17] Consequently, it should be kept in mind that what constitutes a 'normal' waveform (and so what counts as a 'deviation') is mechanism dependent.

Case B (irreproducibility scan-to-scan)

Irreproducibility can be a frustrating part of cyclic voltammetry – why should the same solution and same electrode give different responses in subsequent scans after stirring? In some cases, the electrode is simply modified or passivated during electrocatalysis by a non-catalytic species, resulting in changes to the surface area or morphology, perhaps even changing the heterogeneous electron transfer coefficient for electron transfer to the catalyst ($k°$).[16,22] For example, electrochemical reduction of Brønsted acids by glassy carbon electrodes can generate an insulating film which decreases the heterogeneous electrochemical rate constant and leads to wild variability when the same working electrode is used without intermittent polishing.[20] In extreme cases, severe surface contamination or 'fouling' occurring during a single scan can result in inconsistent CVs even when freshly polished electrodes are used for each trial. In all cases, it is good practice to always start with clean electrodes before any measurements.

For very surface-sensitive electrochemistry, natural variation in electrode surface structure can lead to variability. For example, the glassy carbon "surface structure is often unknown and can vary from laboratory to laboratory or day to day."[23] *Rigorous and consistent surface preparation is essential to obtain rigorous and consistent electrochemical data* (in the words of Jean-Miche Savéant, "the two most important things in electrochemistry are polishing and polishing"‡). One test for surface sensitivity is to evaluate whether there is a significant change in $k°$ when the surface is purposefully modified, for example by covalently bonding nitrophenyl groups to glassy carbon electrodes.[24] No change in peak separation or $k°$ indicates that electron transfer occurs with equal efficacy for both materials, providing evidence that surface sensitivity is not the source of reproducibility challenges.

Irreproducible reaction kinetics are also strong evidence for precatalyst transformation as the kinetic parameters associated with formation of the active catalyst may be complex enough to give wild variation scan-to-scan.[9] This is particularly true if the active catalyst is actually heterogeneous, or has a heterogeneous intermediate,[19] as nucleation in solution or on an electrode surface is extremely difficult to control between experiments. This can lead to sizable fluctuations in the size and amount of heterogeneous catalytic particles generated during the CV.[9] As the potential and magnitude of the catalytic wave depends on how much catalyst has formed at that point in the scan, these fluctuations can lead to significant variation between scans. Observed catalytic rate constants will likely differ between different sizes of heterogeneous catalytic particles, leading to further variability in the waveform. Importantly, this type of irreproducibility may be missed during preparative-scale experiments run at potentials significantly more negative than the catalytic wave.

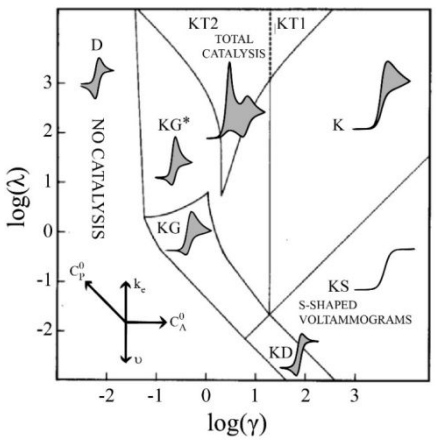

Figure 2. Simulated CV waveforms for how electrocatalysis by a molecular homogeneous can appear. This KZD and simulated CV waveforms specifically describe the one-electron reduction of substrate A via redox catalyst mediator P, where λ is the kinetic parameter and γ is the excess factor. The compass rose visually depicts how catalysis may move between zones (C_P^0 is the initial concentration of catalyst, C_A^0 is the initial concentration of substrate, ν is the scan rate, and k_e is the rate constant for homogeneous electron transfer from the reduced catalyst to the substrate). Reprinted with permission from reference [15]. Copyright 2014, American Chemical Society.

Case C (unexpected diffusional peak)

For a one-electron, one-substrate catalytic reaction, the KZD indicates that the return feature for the redox-triggering event will only be observed on the reverse scan when there is a build-up of reduced or oxidized catalyst (the result of slow reaction rate constants) or complete consumption of substrate (the result of fast reaction rate constants, low substrate concentration).[21] An unexpected diffusion-controlled (generally asymmetric) peak indicates a new homogeneous species was generated during catalysis. For multi-electron catalytic systems, additional return features can provide information on the buildup of catalytic intermediates, such as the oxidation of metal hydride intermediates in H_2 evolution catalysis.[18] This peak could also be the result of oxidation or reduction of the catalytic product, a species formed from catalyst decomposition, or even a redox feature of the true catalytic species.

Case D (unexpected symmetric peak)

Symmetric waves are highly suggestive of redox events arising from surface-adsorbed species.[25] If a new and suspiciously symmetric peak is observed, scan rate (υ) analysis of the background-subtracted peak current can provide a second test for the phase of the species: the peak current will linearly depend on $\upsilon^{1/2}$ for homogeneous species and υ for electrode-adsorbed species. The range of applicable scan rates that can be used is limited by the rates of degradation and, for surface-bound species, deposition onto the electrode. If the rate constant of the chemical reaction or adsorption is slow compared to ν, the current on the return feature will be reduced in magnitude relative to its theoretical value. For reductive catalysis (*e.g.* H_2 generation from acid), symmetric oxidative waves can be 'stripping' waves corresponding to the oxidation of elemental metal plated onto the electrode surface, leading to its desorption from the electrode surface. Highly reducing and protic conditions have been reported to decompose metal complexes into elemental surface-adsorbed metal.[25,26]

Case E (curve crossing)

An initial induction period prior to catalysis is a particularly compelling sign of *in situ* generation of the active catalyst because it implies that catalytic activity has increased as a function of time (see below).[27] In a CV, this induction period can manifest as "curve crossing" where the current on the return scan is higher than the current on the forward scan. Curve crossing stems from the increasing concentration of active catalyst – and so higher catalytic current – as the CV progresses.

Case F (prewave)

Perhaps the most reliable indication of precatalyst transformation is the appearance or existence of an irreversible prewave prior to the catalytic wave in the presence of substrate (**Figure 3**).[10,26,28–31] In some cases, the electrochemically induced chemical reaction that transforms the precatalyst into the active species does not immediately lead to catalysis. If the voltage required for precatalyst transformation is more positive (for reductive catalysis) or negative (for oxidative catalysis) than the catalytic onset potential for catalysis by the active species, then the CV will contain a prewave – *corresponding to formation of the active catalyst* – prior to the catalytic wave. The potential of this prewave can differ drastically from the potential of the precatalyst's reversible $E_{1/2}$ and is directly influenced by the kinetic parameters of the irreversible chemical reaction that follows electron transfer to produce the active species.[32] When the chemical step that generates the active catalyst is slow, the potential of the prewave will be similar to the precatalyst's $E_{1/2}$ (**Figure 3**, red trace). Increasing the observed rate constant for the irreversible chemical step leads to a positive (for reductive processes) or negative (for oxidative processes) potential shift for the prewave, with some features showing peak shifts of hundreds of millivolts with respect to the redox feature of the precatalyst (**Figure 3**, blue trace).[28] In some cases, information about the degradation mechanism can be gleaned from careful analysis of the peak shift magnitude.[28] One caveat when evaluating prewaves is that the degree of reversibility depends on the rates of degradation and thus it may be possible to outcompete the chemical reaction – thereby changing the observed reversibility of the prewave – by varying scan rate or switching potential.

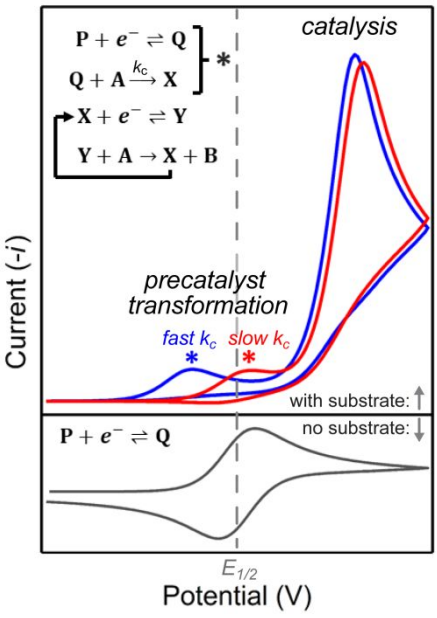

Figure 3. Examples of how prewaves in simulated cyclic voltammograms. Bottom panel contains a simulated CVs of a precatalyst in the absence of substrate undergoing reversible electron transfer (black trace). The top panel contains simulated CV of the conversion of precatalyst to active catalyst when the $E_{1/2}$ of the X/Y couple is 0.2 V negative of the P/Q couple. The red and blue asterisks (*) denotes the prewave associated with irreversible transformation of the precatalyst into the active catalyst when the rate of the chemical step is slow (k_c = 500 M^{-1} s^{-1}, red trace) and fast (k_c = 1x10^{-6} M^{-1} s^{-1}, blue trace), respectively. Chemical and electron transfer steps shown in the panels correspond to the simulated CV(s). Electron transfers were set at 1 cm s^{-1} with α = 0.5, catalytic chemical steps as 1 x 10^6 M^{-1} s^{-1}, concentration of species P and substrate A as 0.5 and 5 mM, respectively, scan rate as 0.1 V/s, and diffusion coefficients of all species as 1 x 10^{-5} cm^2 s^{-1}. Simulated using *DigiElch 8*.

Though irreversible prewaves are a common motif in electrochemical precatalyst transformation, they have also been observed in the catalytic CVs of molecular catalysts in the absence of degradation reaction. This behavior can occur when a very stable catalytic intermediate is formed, such as has been previously observed during CO_2 reduction by iron porphyrin derivatives bearing phenolic functionalities.[13]

Part 2. Assessing if Catalysis is Heterogeneous

When precatalyst transformation generates a heterogeneous catalyst or catalytic intermediate, the electrode itself is often a non-innocent actor in the formation of active species by serving as a template for heterogeneous particle nucleation and growth. Though this reality can be exceedingly frustrating, it has at least one silver lining: a finite area for researchers to check for the possibility of a newly

formed catalyst. As such, numerous methods have been developed to detect and characterize electrode deposits. The most commonly used methods generally rely on post-mortem characterization of an electrode that has been rinsed to remove residual solution, procedures which are effective when the deposited material is stable and strongly bound to the electrode. However, weakly adsorbed products can readily desorb or re-dissolve when rinsed or when not maintained in a specific potential-pH range, rendering these routine tests ineffective. Increasing awareness of metastable catalytic material has fueled interest in developing alternative methods for detecting electroprecipitation.[10,33] In addition to stability to the rinsing process, ex-situ analyses necessitate that the material is stable to the conditions it is exposed to prior to analysis (e.g., pH, atmosphere, vacuum, potential, mechanical handling). This section will discuss currently available methodologies, outlining the conditions in which they are applicable as well as their pitfalls.

It should be stressed that a lack of qualitative evidence in a catalytic CV (as discussed in **Part 1**) is insufficient to rule out precatalyst transformation and researchers are *strongly encouraged* to perform the more rigorous tests discussed in **Part 2**. Indeed, the sometimes-furtive nature of precatalyst transformation can result in initial misidentification of the active catalyst if a full range of methods is not employed. **Table 1** summarizes the methods discussed here and provides literature references for further reading. Given the limited space of this article, we were unable to include all the work and methods applied in the field thus far.

Table 1. Summary of the techniques detailed in Part 2.

method	select literature examples
rinse tests	7,10,25,26,28,30,34,35
mercury poisoning	7,9
induction periods	10,36,37
electrode surface analysis (including SEM, TEM, XPS, AES, AFM, and EDS)	9,26,28,38
electrochemical quartz crystal microbalance	33,39
rotating ring-disc electrochemistry	10,39
spectroelectrochemistry	40

Rinse Tests

Rinse tests are the most common method for detecting *in situ* formation of a heterogeneous or heterogenized active catalyst.[7,10,25,26,28,30,34,35] Two primary variants exist. In the first (**Figure 4**), a CV or linear sweep voltammogram (LSV) is taken with a freshly polished electrode in a solution of catalyst and substrate – the scan is started prior to any redox features and is stopped after scanning through a prewave or the suspected catalytic peaks. This electrode is rinsed with neat solvent and then used to perform an identical scan in a substrate-only solution. If no strongly adsorbed, heterogeneous catalyst has been generated, then no current beyond background will be observed. Presence of any additional current after rinsing – especially anything that looks catalytic – beyond background is strong evidence that at least a portion of the catalytic response is due to an electrode adsorbed active catalyst. Control experiments in which the electrode is first scanned in a catalyst-only solution, rinsed with neat solvent, and used to collect an identical scan in substrate-only solution can help determine if substrate is necessary for electrodeposition.[26]

The second variant involves performing a bulk electrolysis under catalytic conditions – sometimes using a large surface area electrode, such as a glassy carbon plate or reticulated vitreous carbon foam. After the catalytic run, the electrode is rinsed with neat solvent and used to perform another bulk electrolysis in substrate-only solution. Quantification of the amount of current passed, relative to background, as well as the amount of product formed (*e.g.* through headspace analysis for volatile products), allows a surface-adsorbed species to be detected and its catalytic activity quantified. Analysis of the resulting solution should be performed in conjunction with these rinse tests as the film may desorb upon application of a potential or, in the case of metastable films, when it is moved to the analyte-only solution.[19] In these cases, the deposits will diffuse into the solution used for the second

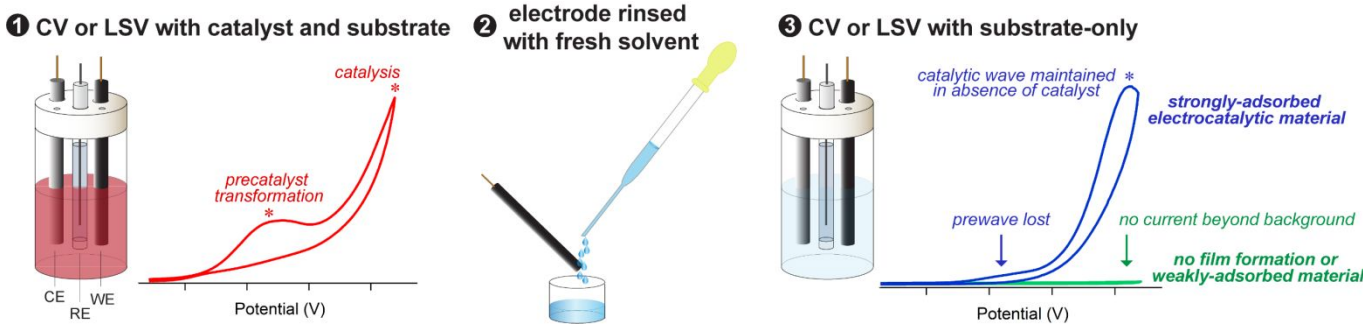

Figure 4. Illustration of procedure and anticipated results for the first primary rinse test variant. A typical three-electrode set-up containing a working electrode (WE), counter electrode (CE), and reference electrode (RE) is used to collect a CV or LSV in a solution of catalyst and substrate. In this example, two voltammetric features can be observed: a catalytic wave preceded by a prewave which corresponds to precatalyst transformation (see **Part 1**). After collecting the CV or LSV, the WE is disconnected and rinsed with fresh solvent to remove soluble components that are only weakly physiosorbed to the surface. A second CV or LSV is then run using the same electrode under the same conditions in a substrate-only solution. If a strongly adsorbed electrocatalytic material was generated in step 1 (blue trace), then a catalytic response will be observed in the substrate-only solution with concomitant loss of the prewave feature. If no electrocatalytic material is generated or the electrode-bound species is removed during rinsing (green trace), then the CV in the substrate-only solution will resemble that of a freshly polished electrode.

bulk electrolysis either as nanoparticles or a molecular species. At sufficiently high concentrations, soluble diffusional products can be detected and characterized. Certain techniques, such as UV-vis absorbance spectroscopy and electrochemistry, can be done without separation of the product from electrolyte while others, such as NMR and mass spectrometry, may be hindered by the presence of electrolyte. Dynamic light scattering can be used to detect the diffusion of nanoparticles into solution.[7]

Though it has been generally assumed throughout this text that heterogenization of the added species requires application of a potential, in reality, the convoluting role of the electrode as a nucleation template means that simply the presence of a certain type of electrode can lead to deposition without any further chemical transformation, as is seen for some metal complexes with aromatic ligands in the presence of graphitic electrodes.[41] To probe this, the previously described rinse tests can be modified such that the electrode is initially soaked in a catalyst-only solution or a solution of catalyst and substrate without an applied potential.[19,37] Performing these rinse tests with different types of electrodes can help determine if this process can be circumvented and what type of chemical reactivity instigates adsorption.[42]

Two potential pitfalls of traditional rinse tests when evaluating metastable species are (1) rinsing can lead to desorption and (2) a species may re-dissolve if left to equilibrate in a solution outside its stable pH-potential range. The amount of catalytic activity observed in the analyte-only solution will depend on the extent of corrosion, a factor which may vary depending on the size and amount of catalytic particles as well as the geometry of the electrode. In extreme cases, the electrode will lose all catalytic activity and rinse test results similar to that of a freshly polished electrode will be observed, *Consequently, a negative rinse test result does not immediately rule out the possibility that the true catalyst is a heterogeneous material*. Modifying the traditional rinse test to avoid these conditions can permit detection of metastable material. In "dry tests", the electrode is quickly removed after scanning in the catalyst/substrate solution *before* the potentiostat begins re-equilibration to the open circuit value. The electrode is then dried and immediately scanned in an substrate or electrolyte-only solution.[10] Great caution should be taken when interpreting the results from dry tests. Because the electrode is not rinsed, residual soluble species may stay attached to the electrode and be transferred to the analyte-only solution. An additional challenge is the time constraints imposed by possible dissolution of the film in the analyte-only solution.

Mercury Poisoning

Collecting a catalytic CV with a Hg-pool working electrode is another control experiment for detecting heterogeneous catalysts. Certain metal particles are inactivated in the presence of Hg(0) through adsorption or amalgam formation; therefore a loss of catalytic activity when using a Hg-pool electrode is a clear indication that metal particles are the active species.[7,9] This protocol is most effective for detecting metal particles made from Pt, Pd, and Ni as they easily amalgamate, but less so for more difficult-to-poison particles such as those derived from Ir, fRh, Ru, and Fe.[7] It is important to check that the added species and other key components do not react with Hg(0).

Induction Periods

Kinetic abnormalities are extremely compelling evidence that the active catalyst is generated *in situ*.[7,9] One quintessential kinetic phenomena of precatalyst-to-catalyst conversion is an initial induction period followed by a rapid increase in catalytic activity. For an induction period for a heterogeneous or heterogenized species to be observable, initial nucleation must be slow and subsequent surface growth fast.[9] In electrochemical assays, induction periods may also result from a buildup of heterogeneous or heterogenized active catalyst on the electrode as more precatalyst diffuses to the surface.[10,36]

As mentioned in **Part 1**, an induction period will manifest in a CV as curve crossing.[37] Induction periods can also be detected using controlled potential methods. In a chronoamperometry experiment, the applied electrode potential is stepped from a voltage where no redox events occur to a potential on the catalytic wave and the current is measured as a function of time (t). For a homogeneous species in the absence of substrate, a diffusion-controlled current is obtained which initially spikes before exhibiting a decay proportional to $t^{-1/2}$.[38] For homogeneous electrocatalysts, addition of substrate results in the passage of more current (red trace, **Figure 5**) compared to the catalyst-only solution ($P + e^- \rightleftharpoons Q$, black trace, **Figure 5**) as the homogeneous chemical reaction regenerates catalyst ($Q + A \rightarrow P + B$). If substrate concentration is in excess, the catalytic current will plateau,

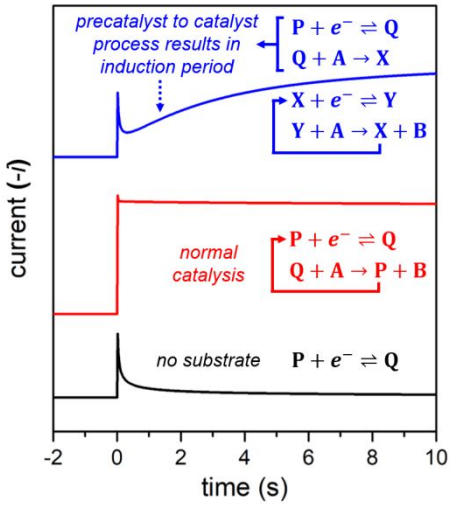

Figure 5. Simulated CAs of a catalyst without substrate (black trace), catalyst with substrate undergoing simple redox catalysis (blue trace), and conversion of precatalyst to active catalyst (red trace). Reaction sequences shown in figure are color-coded to correspond to their simulated CA. Electron transfers were set as 1 cm s^{-1} with $\alpha = 0.5$, catalytic steps with a rate constant of 100 M^{-1} s^{-1}, species P concentration as 1 mM, substrate A concentration as 500 mM, diffusion coefficients of all species as 1 x 10^{-5} cm^2 s^{-1}, rate of $Q + A \rightarrow X$ as 1 M^{-1} s^{-1}, the potential step as 0.3 V negative relative to the $E_{1/2}$ of the P/Q couple, and the X/Y couple as 0.1 V positive relative to the P/Q couple. Simulated using *DigiElch 7*.

otherwise a current decay will be observed as the substrate in the diffusion zone is depleted. For precatalyst transformations with an experimentally observable induction period that occurs on shorter time scales (blue trace, **Figure 5**), an initial current spike will be observed followed by decay due to reduction or oxidation of the precatalyst ($P + e^- \rightleftharpoons Q$). Subsequent degradation of the electrolyzed product ($Q + A \rightarrow X$) to generate the active catalyst then leads to a rise in current attributed to catalysis ($X + e^- \rightleftharpoons Y$, $Y + A \rightarrow X + B$). Observation of this sort of an induction period are expected to lead to lower than 100% Faradaic efficiency as some electrons are lost to generation of the active catalyst.

Additional experimental opportunities are available when a surface-adsorbed electrocatalyst is generated during a prewave. CA experiments in which the potential is stepped to a voltage on the prewave can provide insight into catalyst nucleation and growth if electrodeposition of the active catalyst increases the electrode's total electroactive surface area. This reactivity will lead to a peak-shaped CA where the initial spike/decay is followed by a rapid increase in current associated with the effective increase in electrode surface area and a subsequent decay as film growth becomes diffusion-limited.[22,36]

Currently, CA is rarely used to detect induction periods; we suggest that this simple experiment is an easy check that does not require additional instrumentation. An important caveat for CA with non-hydrodynamic electrodes is that at longer experimental timescales (t > 10 seconds after the potential step) convective mass transport can elevate current relative to theoretical models based on diffusion-limited mass transport.[38] Hydrodynamic methods such as rotating disc electrochemistry (RDE) can help overcome these mass-transport limitations.[36]

Tracking product generation as a function of time during bulk electrolysis experiments can also be used to detect induction periods by noting temporal delays in product formation. In these experiments, it is important to sample multiple early time points. For gaseous products (or reagents), gas chromatography-coupled electrochemical set-ups, rotating ring disk techniques, and Clark electrodes can provide a means for continuous sampling of product formation.[10,39].

Electrode Surface Analysis

Heterogeneous deposits or heterogenized molecular species on electrode surfaces can be directly probed using a variety of analytic methods. Sample preparation will depend on the conditions required for deposition, which can be determined using rinse tests. After deposition onto the surface, the electrode is rinsed (for strongly adsorbed materials) or dried under N_2. These experiments generally use large surface area electrodes, such as glassy carbon plates. RDE shafts with removable disc electrodes can be helpful if hydrodynamic conditions are required for film preparation. Microscopy methods such as scanning electron microscopy (SEM) and transmission electron microscopy (TEM) allow visual detection of surface-adsorbed material.[9,38] These techniques can be used to determine whether the deposited material is a smooth film or discrete nanoparticle deposits.[26,28] They can also provide information on the thickness of the material. Spectroscopy methods such as X-ray photoelectron spectroscopy (XPS), grazing angle FTIR, energy-dispersive XPS (EDS), and Auger electron spectroscopy (AES) allow the elemental composition of the deposited material to be probed, though unequivocal characterization of the electrode-adsorbed material is rarely possible using these methods.[7] These techniques can also provide insight into oxidation states and, in the case of molecular deposits, the morphology of the species.[19,43] Atomic force microscopy (AFM) coupled with time-controlled CA can sometimes help track the growth of catalytically active heterogeneous islands, providing information on the mechanism of nucleation and growth.[36]

The sample preparation methods that we have described are for *ex situ* characterization of the electrode surface. While this method is valuable for strongly adsorbed material, it precludes analysis of weakly adsorbed species. However, there has been a major push to couple many of these techniques with electrochemical measurements (a topic beyond the scope of this review) which – if made widely and easily available – would make them powerful methods for *in situ* characterization of these deposits.

Electrochemical Quartz Crystal Microbalance (EQCM)

EQCM has only recently begun to garner attention as a means of distinguishing between homogeneous (molecular, dissolved) and heterogeneous, electrode-adsorbed electrocatalysis.[33,39] This extremely sensitive technique can allow the deposition of sub-monolayer amounts of material – on the order of nanograms per square centimeter surface area – to be detected during an electrochemical experiment. The goal of this section is to discuss EQCM as it relates to homogeneous molecular electrocatalysis and will include only a brief discussion of the intricacies of this tool; readers interested in a more thorough explanation of the fundamental underpinnings of EQCM are encouraged to explore additional resources.[38,44]

In a typical experimental setup, metal electrodes are deposited on the upper and lower surfaces of a thin quartz crystal which is then positioned in the EQCM cell such that only one side of the crystal is in contact with solution. The conducting surface that is immersed in solution serves as the working electrode during electrochemical measurements. The two electrodes establish an alternating electric field across the crystal, inducing vibration of the crystal at its resonant frequency. During electrode polarization, the frequency of oscillation of the quartz crystal is monitored using a frequency counter while the current passed through the EQCM working electrode is simultaneously measured using the potentiostat.

It is important to stress that the EQCM tracks changes in frequency and *is thus not a direct mass sensor*. Instead, surface mass changes due to deposition cause shifts in the frequency of the resonant vibration. In the simplest case, frequency changes are only caused by (and can be directly related to) interfacial mass changes, with the Sauerbrey equation used to precisely quantify the amount of material added to the surface

with nanogram sensitivity.[45] However, great care should be taken when interpreting EQCM data as simple mass changes are only one of the environmental factors which can contribute to frequency shifts. Interference from a number of other sources (for example, nonuniform mass distribution, electrode surface roughness, changes in viscosity of the contacting medium, and small temperature fluctuations) will lead to deviations from the Sauerbrey equation.[44]

Part of the appeal of using EQCM as a means of detecting *in situ* generation of electrode-adsorbed catalysts stems from its sensitivity under electrocatalytic conditions (in some cases with resolution of ±5 ng),[33] its applicability to transient and weakly adsorbed materials, as well as its ability to help pinpoint the potential at which deposition occurs. This method can have additional utility when catalyst formation occurs during a prewave; in the simple case where the Sauerbrey equation does hold, comparing the charge or current passed during the prewave to the observed frequency change can provide insight into the molar mass of the depositing material.[44] While EQCM is a powerful technique for detecting deposition, it cannot differentiate between deposition of noncatalytic species (such as deactivation products or catalytic by-products) and formation of electrode-adsorbed catalyst. As such, EQCM should always be partnered with additional experiments to confirm the catalytic competency of the deposited material.

Rotating Ring-Disc Electrochemistry (RRDE)

RRDE is a powerful tool for *in situ* detection of redox active reaction products which is primarily used to study surface-anchored catalysts.[39] In collection experiments, the product generated by the disk-anchored catalysts are swept to the ring electrode due to lamellar flow. The potential at the ring is chosen so that the catalytic product(s) of interest are reduced or oxidized (i.e. collected), making the current passed at the ring a direct measure of the amount of product generated at the disk.[38] These experiments monitor how ring current (i_R) and disk current (i_D) change in relation to one another. Ring current and disk current can be related by the collection efficiency (N) which quantifies the fraction of product formed at the disk which subsequently flows past the ring electrode, a metric experimentally described using the ratio of the ring current to the disk current ($N = -\frac{i_R}{i_D}$).[38] Before running any experiments, the collection efficiency value of the ideal RRDE must be established using a simple single-electron redox couple.

Analysis of RRDE data becomes more complicated when studying freely diffusing catalysts because i_R could also reflect electron transfer to/from catalytic intermediates and other homogeneous decomposition products. Given the potential complexities when using RRDE for homogeneous catalysis, it is important to ask the following: what species can I detect at a given ring potential? How is a chemical phenomenon likely to influence i_R, i_D, and N for a given ring potential? This technique is most effective when the redox couples of all diffusional species in the catalytic system are known and the likely lifetime of intermediates can be reasonably estimated. Despite these challenges, intelligently designed RRDE experiments have the potential to be a valuable on-line method for detecting precatalyst transformation (**Figure 6**).

Hypothetically, one could track either product formation or catalytic intermediates by appropriately calibrating the potential the ring is held at. Then, depending on the experiment run at the disk electrode, these metrics can be measured either as a function of time or potential. As mentioned above, RRDE can be used to detect induction periods using controlled potential methods. In this collection experiment, the disc is held at a potential on the catalytic wave and the catalytic product is collected at the ring, allowing generation of catalytic product(s) to be tracked as a function of time. Alternatively, product generation can be tracked as a function of potential by performing a LSV with the disc electrode – the scan is started prior to any redox features and is stopped after scanning through the suspected catalytic peaks – while collecting catalytic products at the ring. This experiment can help pinpoint the potential of catalytic onset as scanning through a catalytic wave will result in an increase in both disk and ring current[39] – a function that is particularly useful when trying to differentiate between a prewave and a catalytic feature (**Figure 6-2**).

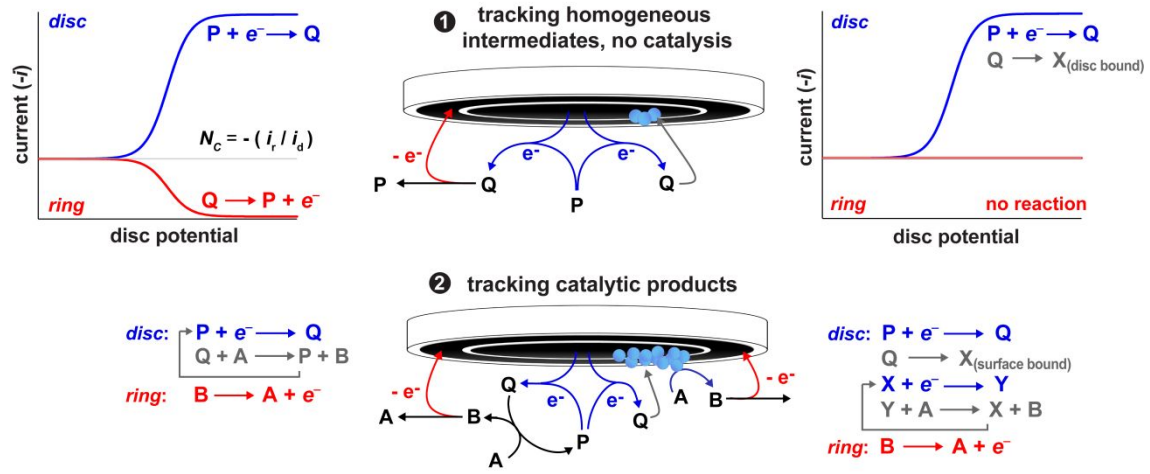

Figure 6. Experimental set-up for RRDE collection experiments. Set-ups based on a one-electron, one-substrate reductive catalytic process. Electron transfer steps to the ring (red) or from the disc (blue) are color-coded. (1) This experiment tracks the production of homogeneous catalytic intermediates in the absence of catalysis. A LSV or CV is collected at the disc (blue trace) which scans through the putative prewave that generates the reduced catalytic intermediate (Q) while the ring is held at a potential where Q is re-oxidized. Ring current is measured as a function of disc potential (red trace). If no deposition occurs (left), the ring current will be related to the disc current by the collection efficiency (N). In contrast, formation of an insoluble species confined at the disc that does not diffuse to the ring will result in no ring current being passed (right). (2) This collection experiment tracks the amount of catalytic product (B) formed during an electrochemical experiment by poising the ring at a potential which re-oxidizes B. This experiment can be used to determine the catalytic onset potential when collecting a CV or LSV at the disc or detect an induction period when running CA at the disc.

Electrodeposition can be directly probed via RRDE if collection of putative diffusional catalytic species can be isolated from collection of product. This prerequisite can be achieved if the surface-adsorbed catalyst is generated during a prewave or if a ring potential can be selected that exclusively measures diffusional catalytic species. In this collection experiment, a LSV is collected at the disc and the ring potential is poised to collect diffusional catalytic species (**Figure 6-1**). If a homogeneous catalytic intermediate is generated, the disc and ring current will increase simultaneously with a *N* similar to that of the ideal RRDE. However, when a redox-induced process generates an insoluble species that is confined to the disc, no product diffuses to the ring resulting in an increase in disk current with no concomitant increase in ring current ultimately leading to a *N* much smaller than that of the ideal RRDE.[10]

Spectroelectrochemistry

Spectroelectrochemistry (SEC) allows spectroscopic and electrochemical data to be intimately coupled by allowing the spectral properties of the electrochemical cell solution to be tracked *in situ* at the surface of the electrode.[38] This can provide similar information to what would be collected by characterizing aliquots from a solution during bulk electrolysis with the added benefit that a smaller solution volume can be used and, for spectrometers that can collect and display data in real time, it allows spectral changes to be directly linked to applied potentials. Experimental set-ups incorporating a wide range of spectroscopic methods have been reported.[32] In our lab, UV-vis SEC has been useful for detecting changes in solubility: generation of a heterogeneous or heterogenized species generally manifests in the UV-vis spectra by a complete loss of defined features and, in some cases, an increase in background absorbance due to scatter. However, the most suitable couple spectroscopic technique will vary based on the structure of the added species, the catalytic transformation of interest, and the properties of the deposited material. SEC used to test for precatalyst transformations has not seen significant use,[40] though we expect this to change given its utility.

Part 3. Case Studies

To illustrate how the methods discussed in **Part 1** and **2** can be employed to develop a comprehensive picture of precatalyst transformation, we present literature examples showcasing how researchers used these techniques to identify the transformation of a molecular species into active catalysts. Also discussed is recent work which applied these methods to detect a heterogeneous molecular catalytic intermediate. These five case studies illustrate the utility of these methods for detecting precatalyst transformation, provide examples of active catalyst characterization, and outline different approaches for identifying and studying degradation mechanisms. Specifically, we focus on studies related to the H_2 evolution reaction (HER) due to the relative simplicity of this reaction as well as the ability to easily control substrate concentration. However, there are number of excellent examples pertinent to other catalytic transformations in the literature.[7,39] While not discussed here, interested readers are directed to our earlier work discussing the structural moieties within molecular species that may pre-dispose them to decomposition and provides a summary of proton reduction catalysts known to decompose under catalytic conditions.[5]

Case Study 1: The pioneering example of cobalt clathrochelate

Type: *Precatalyst to a heterogeneous, adsorbed catalyst*

Highlights: *pre-waves, electrode surface analysis, rinse tests*

The beginning of this century witnessed a sharp acceleration of efforts to find a cheap molecular

electrocatalyst for aqueous proton reduction.[46] An initially promising 'catalyst' was the boron-capped tris(glyoximato) cobalt chlathrochelate complex $[Co(dpg)_3(BF)_2]^+$ (dpg = diphenylgloxime) (**Figure 7**), first reported in 2008.[47] One puzzling aspect of this system was that the metal center in $[Co(dpg)_3(BF)_2]^+$ is coordinatively saturated, prompting questions regarding how protons interacted with the cobalt center. Spurred by these questions, Anxolabéhère-Mallart et al. further investigated the purported electrocatalytic activity of this complex in acetonitrile and water.[30]

In the absence of acid in acetonitrile, reversible $Co^{III/II}$ and $Co^{II/I}$ waves were observed followed at more negative potentials by an irreversible, six-electron wave assigned to the reduction of the glyoxime ligands (**Figure 8a**). Upon titration of perchloric acid, an apparent catalytic wave was seen to grow on top of the $Co^{II/I}$ reduction, consistent with the expectation of Co^{I}-triggered proton reduction. Two observations during titration of perchloric acid revealed that this first wave is not catalytic (marked prewave 1 in **Figure 8b**): (1) it remained peak-shaped at all acid concentrations and (2) it did not increase linearly with acid, instead asymptotically reaching an upper limit. Furthermore, two additional waves at more negative potentials were observed that continued to increase with increasing proton concentration. Plotting i_p/i_p^0 (i_p = peak height of prewave 1, i_p^0 = peak height of the one-electron Co reduction in the absence of acid) as a function of acid equivalents showed that prewave 1 asymptotically approached an upper limit corresponding to a six-electron exchange (**Figure 8c**).

Given this apparent limiting stoichiometry, the authors concluded that all 6 C=N double bonds of the chlathrochelate ligand undergo hydrogenation. Similar analysis of prewave 2, observed as a shoulder on the catalytic wave, proved challenging due to the overlapping catalytic current. The authors did note that the peak height was compatible with an overall 12-electron, 12-proton transformation, a stoichiometry consistent with the hydrogenation of the six N-O bonds.

Similarities between the catalytic wave of the that tails beyond prewave 2 and that observed in CVs recorded in a solution of the simple cobalt salt $Co(NO_3)_2$ and acid suggested deligation of the cobalt metal centre upon reduction. Prompted by these results, additional experiments were undertaken to determine whether the proton-mediated reductive destruction of $[Co(dpg)_3(BF)_2]^+$ generated a surface-adsorbed heterogeneous catalyst. UV-vis absorbance spectra recorded after bulk electrolysis showed complete bleaching of the absorbance features for $[Co(dpg)_3(BF)_2]^+$, suggesting that deligation was succeeded by electrodeposition. Further evidence for electrodeposition came from rinse tests. A glassy carbon electrode was biased at -0.75 V vs. NHE in a solution of $[Co(dpg)_3(BF)_2]^+$ and acid and subsequently rinsed with acetonitrile. After rinsing, the modified electrode was found to be electrocatalytically active for H_2 production in both an acid-only acetonitrile solution and in water at pH 7. Lastly, SEM images of a glassy carbon foil after electrolysis in a solution of $[Co(dpg)_3(BF)_2]^+$ and acid revealed cobalt-containing nanoparticle deposits across the electrode surface, further supporting that catalysis arose from heterogeneous, adsorbed catalytically active material.

Prior to this high profile case, awareness that electrochemical transformation of a parent homogeneous complex could lead to generation of a heterogeneous active catalyst was largely confined to the water oxidation community.[9] This publication brought similar attention to the proton reduction field. The transformation of molecular cobalt chlathrochelates has continued to be a topic of interest as a model system to further expand understanding the interplay between homogeneous and heterogeneous species in electrocatalysis.[31,48]

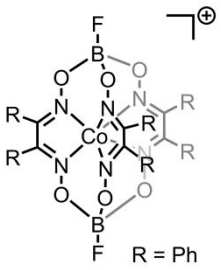

Figure 7. Structure of $[Co(dpg)_3(BF)_2]^+$. Initially reported as a molecular proton reduction catalyst, investigations into how a metal center with a saturated coordination sphere could act as an active catalyst led to the discovery that this species

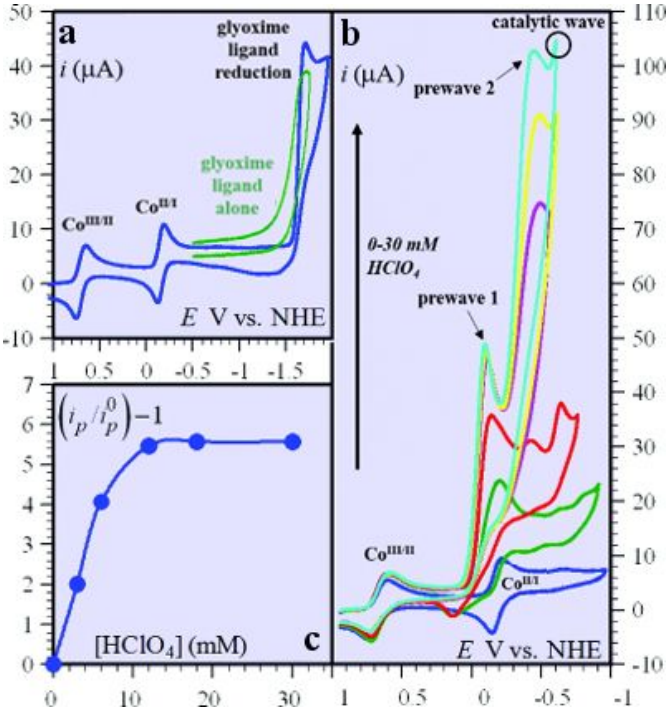

Figure 8. (a) Overlaid CVs of 0.6 mM $[Co(dpg)_3(BF)_2]^+$ and 1.8 mM dpg in 0.1 M $NaClO_4$ acetonitrile solutions. (b) CVs of 0.6 mM $[Co(dpg)_3(BF)_2]^+$ in 0.1 M $NaClO_4$ acetonitrile solutions with 0 mM (blue), 3 mM (green), 6 mM (red), 12 mM (magenta), 18 mM (yellow), and 30 mM (cyan) perchloric acid. (c) Plot of the ratio of the peak current of prewave 1 to peak current in the absence of acid vs. the concentration of added perchloric acid for 0.6 mM $[Co(dpg)_3(BF)_2]^+$ in a 0.1 M $NaClO_4$ acetonitrile solution. Adapted with permission from ref [30]. Copyright (2012) American Chemical Society.

Case Study 2: Linking prewaves to molecular transformations

Type: *Precatalyst to a heterogeneous, adsorbed catalyst*

Highlights: *pre-waves, rinse tests, electrode surface analysis, new symmetric CV waves*

Though prewaves attributed to the chemical modification of a vulnerable ligand moiety was first postulated in 2012 (Case Study 1), evidence supporting such assignments was initially limited to observed electron stoichiometry. C=N and N-O bonds are the most commonly reported structural motifs among molecular precatalysts for surface-adsorbed, H_2-evolution catalysts.[5,28] The vulnerability of these moieties is commonly assigned to hydrogenation for C=N bonds and hydrogenolysis for N-O bonds, with prewaves sometimes invoked as the sole evidence that this mechanism is operative.[29–31,49]

During our evaluation of the H_2-evolving ability of a nickel complex bearing two tridentate ligands with imine functionalities (**Ni(C=N)$_2$**, **Figure 9**), we recognized a unique opportunity to directly probe the chemical transformation occurring during an observed prewave (**Figure 10**, left).[26]

In the absence of acid, the CV of **Ni(C=N)$_2$** in acetonitrile contains two reversible reductions corresponding to the $Ni^{II/I}$ and $Ni^{I/0}$ couples ($E_{1/2}$ = -1.03 and -1.25 V vs $Fc^{+/0}$ (Fc = ferrocene), respectively). Scan rate studies confirmed the homogenous nature of **Ni(C=N)$_2$**.[38] Analogous to the cobalt clathrochelate example in Case Study 1, addition of acid (CF_3COOH) gives rise to two irreversible reductive features – an apparent catalytic wave with an onset near -1.10 V vs $Fc^{+/0}$ and a prewave at -0.98 V vs $Fc^{+/0}$. In addition, an irreversible and fairly symmetric anodic wave appears between -0.10 and -0.60 V vs $Fc^{+/0}$ in the return scan (**Figure 11**). The apparent symmetry of the wave was the key indication that the wave was associated with a surface-bound species as opposed to a new solution species (see **Part 1** above).

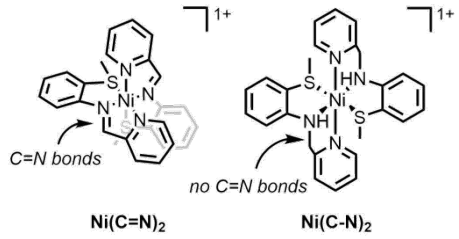

Figure 9. Structures of the proton reduction precatalysts **Ni(C=N)$_2$** and its hydrogenated analogue **Ni(C–N)$_2$**.

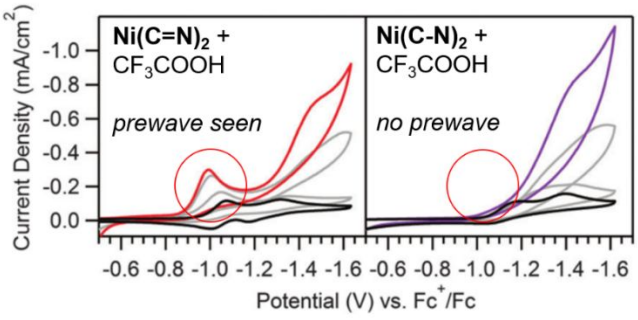

Figure 10. Acid titrations of 0.5, 4, and 10 eq. of CF_3COOH into 0.4 mM solutions of **Ni(C=N)$_2$** and **Ni(C–N)$_2$** in acetonitrile. The black traces are the respective acid- free voltammograms. Adapted with permission from Ref [26]. Published by The Royal Society of Chemistry.

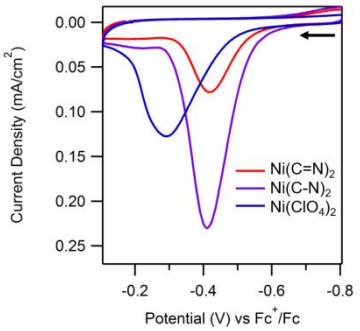

Figure 11. Oxidative stripping waves on the return sweep of CVs of 0.19 mM Ni(C=N)2, Ni(C–N)2, or Ni(ClO4)2 in 0.1 M [Bu4N][PF6] acetonitrile solutions containing 13.6 eq. of CF3COOH. Adapted with permission from Ref [26]. Published by The Royal Society of Chemistry.

Rinse tests and electrolysis experiments coupled with analysis of the electrode surface similar to those in case study 1 confirmed that the homogeneous compound **Ni(C=N)$_2$** decomposed under protic and reducing conditions to form an electrode-adsorbed H_2 evolution catalyst. Characterization via TEM and SEM revealed a Ni/S containing film embedded with nickel-based nanoparticles and the XPS spectra indicated that two distinct Ni species were present. Based on the presence of elemental nickel in the adsorbed material along with the observation that scanning through the symmetric anodic wave led to degradation of the catalytic activity of the film, we postulated that this anodic wave corresponded to stripping of catalytic nickel deposits. A similar anodic feature was observed in the CVs of the simple Ni salt $Ni(ClO_4)_2$, providing strong support for this assignment.

To gain deeper insight into the decomposition mechanism, the stoichiometry of the prewave was established using acid titrations akin to those described in case study 1. Plotting i_p/i_p^0 as a function of acid equivalents showed that the prewave asymptotically approached an upper limit corresponding to the exchange of two electrons per molecule of **Ni(C=N)$_2$**, a stoichiometry consistent with electrochemical C=N hydrogenation of a single ligand.

To provide more concrete evidence for this prewave assignment, a hydrogenated analogue (**Ni(C–N)$_2$**, **Figure 9**) was prepared. CVs of **Ni(C–N)$_2$** in the absence of acid contained a reversible $Ni^{II/I}$ redox couple and, in contrast to **Ni(C=N)$_2$**, an *irreversible* $Ni^{I/0}$ couple. Intriguingly, no prewave was observed in the CV of **Ni(C–N)$_2$** upon addition of acid but an apparent catalytic wave was still observed (**Figure 10**, right). In addition, a similar anodic stripping wave was observed in the CV of **Ni(C–N)$_2$** under catalytic conditions (**Figure 11**).

Motivated by these observations, a series of rinse tests were used to determine the conditions required for electrodeposition of **Ni(C–N)$_2$**. These control studies found that scanning through the irreversible $Ni^{I/0}$ couple in a solution of **Ni(C–N)$_2$** *without acid* was sufficient to generate a heterogeneous, electrode-adsorbed species that is catalytically active for H_2-evolution. Surface analysis by XPS, SEM, and TEM showed that similar decomposition products were generated for **Ni(C=N)$_2$** and **Ni(C–N)$_2$**.

Comparing the redox behavior of **Ni(C=N)$_2$** and **Ni(C–N)$_2$** allowed us to draw two key mechanistic conclusions. First, the lack of prewave in the catalytic CV of **Ni(C–N)$_2$** provides clear evidence that the prewave for **Ni(C=N)$_2$** corresponds to ligand hydrogenation. Second, the acid-independent electrodeposition of **Ni(C–N)$_2$** upon traversing the irreversible $Ni^{I/0}$ feature suggested that reduction of the hydrogenated **Ni(C=N)$_2$** species (**Ni(C=N)$_2$***) generated during the prewave leads to electrodeposition without additional proton transfer.

Case Study 3: Prewave and curve crossing seen for a Ni precatalyst

Type: *Precatalyst to a heterogeneous, adsorbed catalyst*

Highlights: *pre-waves, curve crossing, electrode surface analysis*

Two years after the $[Co(dpg)_3(BF)_2]^+$ study, Roberts *et al.* reported that an initially promising molecular proton reduction catalyst, $Ni(bdt)_2^-$ (**Figure 12**), was in fact a precatalyst for a heterogeneous active catalyst.[37] We will not discuss this paper in extensive detail, but readers are strongly encouraged to review the original report as it is a wonderful example of how voltammetric and spectroscopic data can be coupled to gain a comprehensive understanding of degradation processes.

Two key features in the voltammograms recorded with acid helped the authors suspect that $Ni(bdt)_2^-$ was a precatalyst. The first was an irreversible prewave nearly 200 mV positive of the $[Ni(bdt)_2]^{-/2-}$ redox couple that became quasi-reversible at sufficiently high scan rates, suggesting the corresponding reduction was coupled to a follow-up chemical reaction.

In addition to this tell-tale prewave, Roberts *et al.* also observed curve crossing on the return sweep of their CVs (**Figure 13**). Curve crossing on the return sweep of a cyclic voltammogram is a classic example of more complex downstream reaction chemistry.

Curve crossing was initially mathematically detailed by Savéant *et al.* for electrochemically induced aromatic nucleophilic substitution.[50] In brief, the appearance of enhanced current on the return scan indicates that the forward sweep induced chemical reactions resulting in downstream products with redox couples more positive than the reactant redox couple. Well-established methods exist for understanding the specific mechanism for these electrochemically induced reactions.[8] Curve crossing has also been demonstrated to arise from *autocatalytic* electrochemistry. For aryl thiocyanates, electrode reduction results in generation of a reduced species capable of catalyzing subsequent reduction events; concentration-dependence studies supported the autocatalytic nature.[51]

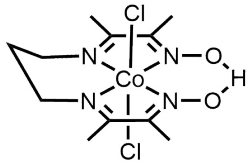

Figure 14. Structure of a cobalt diamine-dioxime complex (abbreviated here as **CoLCl$_2$**), a molecular proton reduction precatalyst.

In this case study, the curve crossing in the catalytic peak demonstrated that the catalytic activity is *enhanced* later in the scan even though the local concentration of substrate – here, protons – was diminished during catalysis on the forward scan. As mentioned in Part 1, curve crossing is a time-dependent feature which is consistent with an induction period required for activation of the precatalyst into the true active species. The presence of a curve crossing is interesting in light of the fact that a well-defined prewave is also observed in the voltammograms.

Motivated by the observation of a prewave and curve crossing upon substrate addition, Roberts *et al.* performed rinse test and surface analysis similar to those described in Cases 1 and 2. These confirmed the generation of an electrode-bound heterogeneous Ni-S species that is catalytically active for H_2 evolution. To dig into the electrodeposition mechanism, the authors carried out a series of rinse tests which varied the electrodeposition potential. These experiments showed that the catalytic response of the film depended in a nonlinear manner on the deposition potential, underscoring how highly sensitive the film structure is to electrodeposition conditions. Based on these results, the authors postulated that deposition must involve one or more reduction steps, which could explain the presence of both

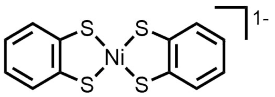

Figure 12. Structure of Ni(bdt)$^-$, a precatalyst for heterogeneous H_2 evolving Ni-S film.[37]

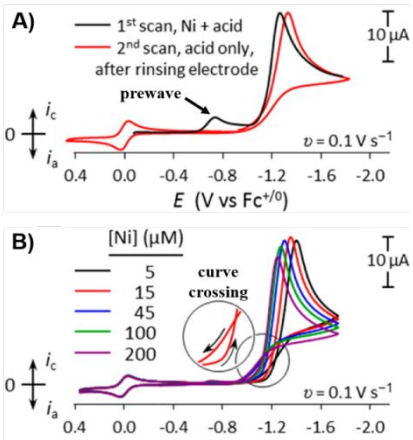

Figure 13. **A)** LSV of 1 mM $[Ni(bdt)_2][Bu_4N]$ with 10 mM $[4\text{-}BrC_6H_4NH_3]BF_4$ in 0.2 M $[Bu_4N][PF_6]$ acetonitrile solution, demonstrating a prewave prior the catalytic wave, and a CV using the same electrode after rinsing in a solution containing only 10 mM $[4\text{-}BrC_6H_4NH_3][BF_4]$. **B)** Voltammograms of varying concentrations of $[Ni(bdt)_2][Bu_4N]$ with 10 mM $[4\text{-}BrC_6H_4NH_3][BF_4]$ showing curve crossing on the return trace. Adapted with permission from ref [37]. Copyright (2014) American Chemical Society.

curve crossing and a prewave.We highlight this paper as one of the few well-defined examples of a molecular precatalyst which was observed to result in curve crossing in catalytic cyclic voltammograms, in addition to the more commonly seen prewave. Researchers who observe curve crossing in their own catalytic cyclic voltammograms are encouraged to review into the key literature references of this section.

Case Study 4: The danger of false-negative rinse tests

Type: *Precatalyst to a heterogeneous, adsorbed catalyst*

Highlights: *pre-waves, dry rinse tests, induction periods, RRDE*

During case studies 1–3, researchers were able to successfully utilize rinse tests to confirm that the nature of the active catalyst was heterogeneous. As mentioned in **Part 2,** an important caveat for routine rinse tests is that *while a positive rinse test is strong evidence for deposition of a catalytically active material on the electrode surface, a negative rinse test is insufficient to rule out electrodeposition*. An electrode-adsorbed species generated under harsh catalytic conditions – *e.g.*, extreme reducing/oxidizing potentials, strongly basic/acidic conditions - may readily desorb or re- dissolve when rinsed with solvent or left to equilibrate in electrolyte solution, leading to a false-negative rinse test.

If a routine rinse test is the sole control experiment used to identify heterogeneous catalysis, a false-negative would lead to misidentification of the active catalyst. Recently, it was realized that the rinse test performed for a putative cobalt-based H_2-evolution catalyst (**$CoLCl_2$**, **Figure 14**) failed to detect metastable catalytic nanoparticles resulting in erroneous identification of the added species as the active catalyst.[52] In follow-up investigations, another team was able to identify the true catalyst using a combination of analytical techniques.[10] This case study highlights experimental pitfalls that can lead to misidentification and provides an excellent blueprint for deciphering the true origin of catalysis.

The catalytic competency of molecular **$CoLCl_2$** was originally evaluated with glassy carbon electrodes using RDE and chronocoulometric measurements.[52] RDE voltammograms of **$[CoL(H_2O)_2]^{2+}$** in aqueous phosphate buffer (pH = 2.2) contained an irreversible reductive feature (onset = -0.26 V vs RHE) with a plateau current seven-times that of the one-electron $Co^{III/II}$ wave which was assigned to catalytic H_2-evolution mediated by the molecular species **$CoLCl_2$**. Assessing catalytic activity over a wide range of acidic to neutral aqueous buffers solution showed a 60 mV per pH unit shift of this putative catalytic wave. Bulk electrolysis at -0.56 V vs RHE – a potential far more negative than the putative catalytic wave – confirmed H_2 production with 80% faradaic efficiency. The solution underwent a suspicious color change during the 2-hr electrolysis experiments, irreversibly changing from yellow to colorless. Though formation of a heterogeneous, surface-adsorbed catalyst was considered as an explanation for the observed color change and sub-unity faradaic efficiency, this possibility was rejected on the basis of rinse test results. After electrolysis experiments in a solution of **$CoLCl_2$**, the electrode was rinsed with water and a second electrolysis experiment was run in electrolyte solution. The charge passed by the rinsed electrode was similar to that of a freshly polished electrode, leading the authors to exclude heterogenous catalysis.

This initial report drew the attention of Artero and co-workers who had developed a hybrid electrocatalytic material in which **$CoLCl_2$** was covalently attached to a multi-walled carbon nanotube deposited onto a gas diffusion layer (GDL/MWCNT-[**$CoLCl_2$**]).[53] This material was reported to sustainably evolve H_2 in aqueous acetate buffer (pH = 4.5). Interested in the original pH dependence reported, they evaluated their hybrid material in aqueous phosphate buffer (pH = 2.2) using LSV coupled with in-line quantification of H_2 production using gas chromatography to determine if more acidic conditions would be beneficial for catalytic activity.[10] During these evaluations, they noticed that the voltammetric onset potential for GDL/MWCNT-[**$CoLCl_2$**] was over 200 mV higher than that of homogeneous **$CoLCl_2$** with glassy carbon electrodes under the same conditions. The pH-dependence of catalytic onset also differed – with the catalytic wave of GDL/MWCNT-[**$CoLCl_2$**] displayed similar overpotentials at pH 4.5 and 2.2.[53] In addition, the shape of the electrocatalytic waves for **$CoLCl_2$** appeared more Nernstian that that of the GDL/MWCNT-[**$CoLCl_2$**]. These inconsistencies were the first indications that the catalytically active species were not the same in both systems.

The authors next investigated the electrochemistry of *dissolved* **$CoLCl_2$** in aqueous phosphate (pH = 2.2) buffer using a GDL/MWCNT working electrode to determine whether these inconsistencies were simply the result of differences in the electrode material. Four reductive events could be resolved in the CVs of **$CoLCl_2$** when very low scan rates (0.1 mV s^{-1}) were employed: feature **A** (+0.49 V vs RHE) corresponding to the $Co^{III/II}$ couple, overlapping features **B_1** (onsets = ca. -0.20, inflection point = -0.33 vs RHE) and **B_2** (onsets = ca.-0.40 vs RHE), and a large wave **C** (-0.93 V vs RHE). They note that the potential of wave **B_1** is strikingly similar to the catalytic feature described in the original report when similar measurements were performed with dissolved **$CoLCl_2$** on a glassy carbon

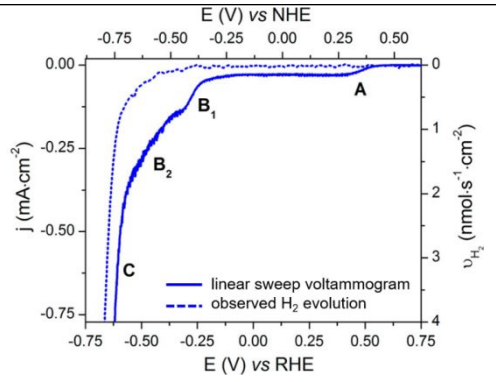

Figure 15. Comparison of the LSV of **$CoLCl_2$** in pH 2.2 aqueous phosphate buffer at 0.1 mV/s with a GDL/MWCNT electrode with the real time *in situ* observed H_2 evolution, demonstrates that the initial redox features **A**, **B_1**, and **B_2** do not correspond to proton reduction catalysis. Adapted with permission from ref [10]. Copyright (2016) American Chemical Society.

working electrode. The H_2 evolution rate was tracked during these scans using in-line GC monitoring in order to determine when catalysis truly began (**Figure 15**).

The current density and H_2 evolution rate for homogeneous **$CoLCl_2$** using GDL/MWCNT electrodes differed significantly from those measured with the GDL/MWCNT-[**$CoLCl_2$**] hybrid material. For GDL/MWCNT-[**$CoLCl_2$**], the GC-coupled electrochemical set-up showed current onset at approximately -0.51 V vs RHE with concomitant H_2 production. For homogeneous **$CoLCl_2$**, H_2 evolution was observed at approximately -0.40 V vs RHE – *corresponding to the onset of wave* ***B_2***. This was particularly striking to them because it suggested that feature **B_1** is in fact a prewave that could correspond to the formation of the true active species.

Questioning the true nature of the catalytically active species, they turned to surface characterization. Analysis of the unmodified GDL/MWCNT electrodes after cathodically scanning in the **$CoLCl_2$** solution by field electron gun-SEM and XPS revealed cobalt-containing nanoparticles on the surface of the tube. For modified electrodes that had been rinsed with water for a few seconds post-LSV, fewer cobalt-based nanoparticles were observed. Rinsing also reduced the size of the remaining nanoparticles and modified their shape, leaving only the core of the particles on the electrode surface. To evaluate the catalytic activity of these deposits, dry tests were performed in which a cathodic sweep of **$CoLCl_2$** was obtained using a GDL/MWCNT electrode. After the LSV, the electrode was quickly disconnected, dried under N_2, and then immediately used to scan in a fresh phosphate buffer electrolyte solution (pH = 2.2) with simultaneous GC monitoring. H_2 evolution started at -0.40 V vs RHE – a potential similar to that for the onset of **B_2**.

After identifying precatalyst decomposition on GDL/MWCNT electrodes, Artero and coworkers set out to determine whether glassy carbon displays similar reactivity. RRDE experiments were performed for a solution of **$CoLCl_2$** with a glassy carbon disk and a Pt ring. This setup allowed them to track product formation which could be directly compared to the initial RDE experiments. The ring potential was set such that both H_2 and any reduced cobalt complexes generated at the disk would be re-oxidized. Features **A** and **C** were readily identifiable in the LSV collected at the glassy carbon disk, however redox features **B_1** and **B_2** could not be resolved and instead a single feature **B** was observed in this potential range. Features **B_1** and **B_2** could, however, be differentiated at the ring due to changes in collection efficiency. Collection efficiency remained constant when scanning through **A** and **B_1**, indicating that only soluble reduced compounds are generated at these potentials. Upon scanning through **B_2**, the ring current dropped significantly, suggesting generation of an insoluble species that adsorbs the disk and cannot be swept to the ring. A steep increase in ring current was observed at wave **C**; this was attributed to H_2 production catalyzed by the newly adsorbed species.

Electrolysis experiments at five potentials (-0.14, -0.45, -0.52, -0.57, and -0.65 V vs RHE) were conducted using stationary glassy carbon plates. GC monitoring confirmed that

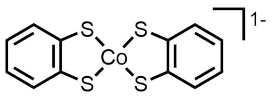

Figure 16. Structure of $Co(bdt)_2^-$.

H_2 production does occur at **B** (-0.45 V vs RHE), *but only after the first 5-minutes* and with a faradaic yield of only 27%, implying proton reduction is not the dominant process. For the potentials throughout the course of wave **C** (-0.52, -0.57, and -0.65 V vs RHE), a similar 5-minute induction period was observed followed by proton reduction catalysis with faradaic yields of 40, 70, and 80%, respectively.

Surface characterization was then conducted after preparative scale electrolysis at -0.57 V vs RHE. If the glassy carbon plates were rinsed, SEM and EDX results were similar to that of a pristine electrode. However, if the plates were instead quickly disconnected after the LSV and dried under N_2, Co-based deposits of various shapes were observed. Similarly, glassy carbon electrodes prepared in the same manner lost almost all catalytic activity if they were rinsed prior to collecting a scan in fresh buffer solution. Even without rinsing, the activity of the deposits in pristine electrolyte is reduced, suggesting that the absence of an applied cathodic potential is sufficient to decrease the stability of the cobalt-based nanoparticles.

From these data, Artero and coworkers were able to map out a mechanism of degradation and electrodeposition. Of particular importance was the recognition of wave **B_1** – a feature that could not be resolved using glassy carbon electrodes - was a prewave as it allowed for more critical analysis of the stoichiometry of this feature. **$CoLCl_2$** has 4 C=N bonds and 2 N-O bonds, both moieties known to be susceptible to degradation. As noted previously, the plateau current for **B** is 7-times that of the one-electron $Co^{III/II}$ wave. This 7-electron stoichiometry is close to the 8 electrons required for hydrogenolysis of the 2 N-O bonds (2 electrons, 2 protons each) and hydrogenation of the two diamine backbones (2 electrons and 2 protons each), leading to the re-assignment of **B_1** to the electrochemical degradation of the diimine-dioxime ligand.

Though electrochemical analysis implicates ligand degradation during prewave **B_1**, ligand degradation did not result in formation of a surface-adsorbed catalyst. The drop in collection efficiency seen in RRDE experiments upon scanning through wave **B_2** indicated that further reduction was required for electrodeposition. This is followed by a drastic increase in ring current upon scanning through wave **C** which was attributed to catalysis. Electrolysis experiments run at potentials throughout waves **B** and **C** all showed a similar induction period, a tell-tale sign of precatalyst transformation, and faradaic efficiency indicated that the catalytically active and electrode-adsorbed species is generated at **B** but actual generation of H_2 occurs at more negative potentials. Unlike previous studies with similar cobaloxime species, traditional rinse tests provided no evidence of electrodeposition, indicating the deposited material is weakly adsorbed.[30] However, the generation of cobalt-based catalytic material

could be confirmed using surface characterization if the film was immediately dried under N_2 and dry tests used to confirm catalytic competency.

This example exemplifies how careful application of different techniques can overcome the limitations of traditional rinse tests and allow detection of metastable material.[10,52]

Case Study 5: Detecting the Homogeneous/Heterogeneous Interplay of a Catalytic Intermediates

Type: *A molecular, adsorbed catalyst intermediate*

Highlights: *irreproducibility, spectroscopy, rinse tests*

Metal dithiolene compounds have garnered considerable attention as H_2-evolution electrocatalysts and as model systems for investigating the elementary steps governing proton reduction.[19,37] Part of this popularity stems from their reactive redox non-innocent ligands. Intrigued by work from McNamara *et al.* describing impressive activity of **Co(bdt)$_2^-$** (**Figure 16**) for electrocatalytic H_2 production, we recently investigated the reactivity of **Co(bdt)$_2^-$** using a series of *para*-substituted aniliniums (4-X-AnH$^+$) in acetonitrile to gain insight into the catalytic reaction mechanism.[19,54] Using many of the techniques discussed above, we identified two parallel catalytic pathways – one which was purely homogeneous, and a second that involved an electrode-adsorbed intermediate.

Unlike previous case studies, the CVs contained no obvious prewaves or curve crossing that implicated an electrode-adsorbed species. Instead, our preliminary analysis of **Co(bdt)$_2^{2-}$** was complicated by irreproducibility – which though frustrating, proved essential for identifying the true nature of a key catalytic intermediate. CVs of **Co(bdt)$_2^{2-}$** in the absence of acid contain a one-electron, reversible wave ($E_{1/2}$ = -1.24 V vs Fc$^{+/0}$) corresponding to the **Co(bdt)$_2^{-/2-}$** couple (**Figure 17**). Upon addition of 0-2 equivalents acid, an irreversible cathodic feature (**A**) was observed at potentials positive of the **Co(bdt)$_2^{-/2-}$** couple. The exact potential of **A** varied with acid identity with decreasing acid pK_a correlating with more positive peak potentials. This behavior is qualitatively consistent with a catalytic CV in the total catalysis regime (KT2) leading us to tentatively assign **A** as a catalytic wave.[8,15]

More rigorous investigation uncovered a large degree of inconsistency in the redox behavior of **Co(bdt)$_2^{2-}$** (**Figure 18a**). Though a general linear trend was observed when plotting the potential of **A** as a function of acid pK_a, both the potential and broadness of **A** varied widely between trials (**Figure 18b**). Analogous studies evaluating the impact of catalyst concentration were similarly plagued with consistency problems. Strikingly, the degree of variability increased with higher catalyst concentration. From these results, we postulated that a secondary process that becomes more acute at higher catalyst loadings was convoluting analysis – *behavior consistent with in situ formation of an electroactive electrode-adsorbed species.*

Initial rinse tests indicated that little-to-no strongly adsorbed material was generated during a cathodic sweep in a solution of **Co(bdt)$_2^{2-}$** and AnH$^+$ (pK_a = 10.62). Fortuitously, two qualitative observations made during trials with stronger acids guided us in the right direction. Optically monitoring a solution of **Co(bdt)$_2^{2-}$** and 4-CN-AnH$^+$ (pK_a = 7) showed a rapid bleaching of the UV-vis signal with concomitant precipitation of black particulates. Further analysis revealed that the rate of precipitation increased with acid strength. Another important observation was the visible discoloration of the electrode when collecting CVs with **Co(bdt)$_2^{2-}$** and 4-Cl-AnH$^+$ (pK_a = 9.7). Based on these results, we postulated that protonation of unreduced **Co(bdt)$_2^{2-}$** leads to the precipitation of black particulates which can adsorb onto the electrode.

To clarify the redox behavior of this film, rinse tests were conducted using electrodes soaked in a solution of **Co(bdt)$_2^{2-}$** and 4-Cl-AnH$^+$ *without application of a potential* before rinsing with acetonitrile. Multiple prominent redox features were visible in the CV of an acid-only solution collected with modified electrodes that had been soaked for 15 seconds. The relative magnitude and number of features evolve as the soak time increases (**Figure 19**), providing one explanation for the previously observed variability.

Glassy carbon plates soaked in a solution of [Co(bdt)$_2$]$^-$ and 1 equivalent 4-CN-AnH$^+$ were analyzed via XPS. The Co 2p region of the film and dropcast **Co(bdt)$_2^{2-}$** both contained one doublet with similar binding energies, indicating that one type of molecular cobalt species is present in both samples. A single doublet is observed in the S 2p region for dropcast **Co(bdt)$_2^{2-}$** confirming that one type of sulfur is present, as expected given the symmetry of the molecule. In contrast, the S 2p region for the film contained a broad feature at a higher binding energy which consisted of multiple overlapping doublets, suggesting a break in molecular symmetry consistent with protonation of one or more sulfur sites. XPS spectra of the insoluble black particles were qualitatively similar to that of the film.

Rinse tests also showed that the surface-adsorbed material readily desorbs upon cycling multiple times in acidic or electrolyte-only solution. To characterize the desorption product generated upon reduction of the film, a modified glassy carbon plate was subjected to reducing potentials in an electrolyte-only solution. UV-vis absorption spectra recorded of the resulting solution showed that molecular **Co(bdt)$_2^{2-}$** had

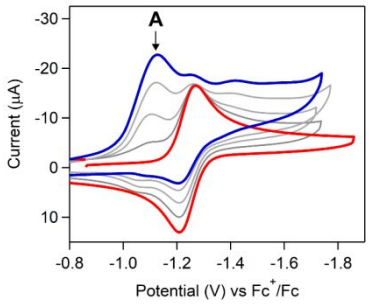

Figure 17. CVs of [Co(bdt)$_2$]$^-$ in the absence of a proton source (blue) and as anilinium (0.5 to 2 eq.) is titrated into solution (grey to blue). Putative catalytic wave **A** falls at potentials positive of the [Co(bdt)$_2$]$^-$ redox couple, consistent with the KT2 regime. Adapted with permission from ref [19]. Copyright (2017) American Chemical Society.

been regenerated, implying the integrity of the molecular core was not degraded during film formation. Chemical reduction of isolated black particulates led to the regeneration of molecular **Co(bdt)$_2^-$**, further suggesting similar identities of the film and particles.

Based on these results, a general catalytic mechanism was postulated in which protonation of unreduced **Co(bdt)$_2^-$** initiates precipitation and film formation. The observed dependence of the rate of precipitation on acid pK_a suggested that two pathways are operative – strong acids that are capable of protonating the unreduced form proceed via a molecular, heterogenized intermediate while a homogeneous, reduction-initiated pathway dominates for weaker acids. Upon reduction, the protonated heterogeneous intermediates is readily converted to molecular **Co(bdt)$_2^-$** with concurrent release of H_2.

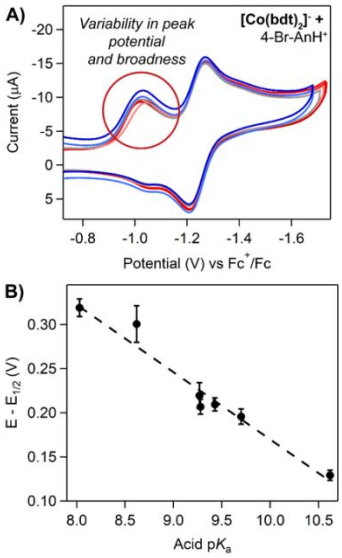

Figure 18. **(A)** CVs of $[Co(bdt)_2]^-$ in the presence of 1 equivalent 4-Br-AnH$^+$ using freshly polished electrodes highlight the irreproducibility from scan to scan. **(B)** Plotting peak potential as a function of acid pK_a shows how irreproducibility convolutes the linear dependence. Experimental averages indicated by black dots along with associated standard deviation and black dashed line indicates the linear fit. Acid identities: An-H$^+$ (pK_a = 10.62), 4-Cl-AnH$^+$ (pK_a = 9.7), 4-Br-AnH$^+$ (pK_a = 9.43), 4-OCF$_3$-AnH$^+$ (pK_a = 9.28), 4-I-AnH$^+$ (pK_a = 9.27), 4-(methylbenzoate)-AnH$^+$ (pK_a = 8.62), and 4-CF$_3$-AnH$^+$ (pK_a = 8.03). Adapted with permission from ref [19]. Copyright (2017) American Chemical Society.

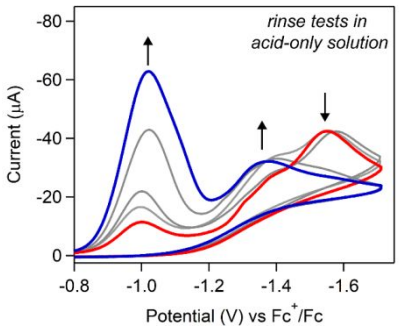

Figure 19. Rinse test CVs of an acid-only solution using electrodes that had been soaked for times ranging from 15 seconds to 10 minutes (red to blue) in a solution of $[Co(bdt)_2]^-$ and acid. Arrows highlight how voltammetric features evolve as a function of time soak time. Adapted with permission from ref [19]. Copyright (2017) American Chemical Society.

In this case study, irreproducibility in catalytic CVs was the first indication that two parallel catalytic pathways – one of which proceeded via a heterogenized intermediate – were operative. This is interesting considering that a purely chemical reaction (protonation) generated the molecular, heterogenized intermediate. When transformation of a homogeneous precursor to a heterogeneous species requires electron transfer (as was observed in case studies 1-4), only the tiny fraction of the precatalyst at the electrode surface will likely decompose during non-destructive electrochemical experiments such as cyclic voltammetry. However, in the case of a purely chemical reaction, precipitation of heterogeneous materials in the bulk solution is also expected and standard techniques which monitor changes to the bulk solution will likely be applicable. Though optical monitoring did eventually allow us to identify particulates, this transformation was only obvious when using more forcing conditions – *e.g.*, strong acids or high acid concentrations. In contrast, formation of this heterogenized intermediate had an obvious impact on the electrochemical data (in the form of irreproducible CVs) under far more mild conditions. This highlights the convoluting role of the electrode as a template for heterogeneous particle nucleation and growth as well as the sensitivity of electrochemical measurements to changes at the electrode surface.

Conclusions

Important strides have been made over the past few decades in the field of molecular electrocatalysis, gains that have been paralleled by the development of new methods of electrochemical analysis which have allowed researchers to gain in-depth insight into catalytic mechanisms and kinetic parameters. The majority of these improvements have been in catalytic activity and selectivity, with the question of how to improve catalyst stability rendered comparatively out of vogue. However, the last decade has seen a slight uptick in the number of reports focused on the topic of catalyst stability, likely spurred by the discovery of numerous examples where initially promising catalysts were, in fact, decomposing and/or transforming *in situ* into new catalytically active species, many of which were heterogeneous in nature. While these new species may be excellent catalysts in their own right, rationally benchmarking and improving catalytic systems requires intimate knowledge of the identity of the active catalyst. This is particularly important when designing *molecular* catalysts as one of the touted benefits of these species is the ability to fine tune catalytic properties through ligand modification.

Thanks to a steadily growing number of papers describing precatalyst transformation, we are now in a position to more rapidly identify electrochemical decomposition of molecular species to generate an active catalyst. A more established library of the tell-tale signs in CVs which suggest precatalyst transformation has been developed, enabling quick triages which can be performed directly using only catalytic voltammograms, as discussed in Part 1 of this Tutorial Review. These suspicious signs can provide qualitative evidence, however more rigorous follow-up should be conducted using

the methods discussed in Part 2 when transformation to a heterogeneous species is suspected. These techniques are particularly valuable because they can both confirm the presence of electrode-adsorbed films and provide important information about the structure and nature of the true active species which can be used to identify the decomposition mechanism via the strategies outlined in Part 3.

In this Tutorial Review, we have attempted to cover a wide range of state-of-the-art techniques. There will doubtless be further refinement of these existing methods and development of new techniques which will hopefully provide greater insight into the factors that contribute to decomposition as well as strategies to avoid unfavorable degradation reactions. The growing recognition of metastable catalytic material has placed increased emphasis on the need to develop methods for evaluating precatalyst transformation *in situ*. It is worth noting that some researchers have found that many of the heterogeneous materials generated by precatalyst transformation are excellent catalyst in their own right, with early studies showing that the nanostructuration or nature of the material can be controlled by the initial design of the ligand. We hope that this review will enable researchers of all stripes to quickly establish the identity of the active catalyst in their own work and that it can prove a helpful guide for those interested in understanding the nucleation and growth of favorable decomposition products.

Conflicts of interest

There are no conflicts to declare.

Footnotes

‡The direct translation from French reads “polishing and sweeping are the two udders of electrochemistry,” but this requires extensive knowledge of French history and Henry IV of France.

Acknowledgements

We are thankful for the many beta readers whose contributions substantially improved this paper. This work was supported by the U.S. Department of Energy, Office of Science, Office of Basic Energy Sciences under Award DE-SC0015303.

References

1 U.S. Global Change Research Program, 2018, **II**, 1–470.
2 R. J. Detz, J. N. H. Reek and B. C. C. van der Zwaan, *Energy Environ. Sci.*, 2018, **11**, 1653–1669.
3 D. L. DuBois, *Inorg. Chem.*, 2014, **53**, 3935–3960.
4 R. Francke, B. Schille and M. Roemelt, *Chem. Rev.*, 2018, **118**, 4631–4701.
5 N. Elgrishi, B. D. McCarthy, E. S. Rountree and J. L. Dempsey, *ACS Catal.*, 2016, 3644–3659.
6 P. Garrido-Barros, C. Gimbert-Suriñach, R. Matheu, X. Sala and A. Llobet, *Chem. Soc. Rev.*, 2017, **46**, 6088–6098.
7 V. Artero and M. Fontecave, *Chem. Soc. Rev.*, 2013, **42**, 2338–2356.
8 J.-M. Savéant, *Elements of Molecular and Biomolecular Electrochemistry*, John Wiley & Sons, Inc., Hoboken, NJ, USA, 2006.
9 J. A. Widegren and R. G. Finke, *J. Mol. Catal. A Chem.*, 2003, **198**, 317–341.
10 N. Kaeffer, A. Morozan, J. Fize, E. Martinez, L. Guetaz and V. Artero, *ACS Catal.*, 2016, **6**, 3727–3737.
11 J. J. Stracke and R. G. Finke, *ACS Catal.*, 2014, **4**, 909–933.
12 G. M. Jacobsen, J. Y. Yang, B. Twamley, A. D. Wilson, R. M. Bullock, M. Rakowski DuBois and D. L. DuBois, *Energy Environ. Sci.*, 2008, **1**, 167.
13 C. Costentin, G. Passard, M. Robert and J. M. Savéant, *J. Am. Chem. Soc.*, 2014, **136**, 11821–11829.
14 C. Costentin, S. Drouet, M. Robert and J.-M. Savéant, *J. Am. Chem. Soc.*, 2012, **134**, 11235–11242.
15 E. S. Rountree, B. D. McCarthy, T. T. Eisenhart and J. L. Dempsey, *Inorg. Chem.*, 2014, **53**, 9983–10002.
16 N. Elgrishi, K. J. Rountree, B. D. McCarthy, E. S. Rountree, T. T. Eisenhart and J. L. Dempsey, *J. Chem. Educ.*, 2018, **95**, 197–206.
17 D. J. Martin, B. D. McCarthy, E. S. Rountree and J. L. Dempsey, *Dalt. Trans.*, 2016, **45**, 9970–9976.
18 E. S. Rountree, D. J. Martin, B. D. McCarthy and J. L. Dempsey, *ACS Catal.*, 2016, **6**, 3326–3335.
19 K. J. Lee, B. D. McCarthy, E. S. Rountree and J. L. Dempsey, *Inorg. Chem.*, 2017, **56**, 1988–1998.
20 B. D. McCarthy, D. J. Martin, E. S. Rountree, A. C. Ullman and J. L. Dempsey, *Inorg. Chem.*, 2014, **53**, 8350–8361.
21 J.-M. Savéant and K. B. Su, *J. Electroanal. Chem.*, 1984, **171**, 341–349.
22 R. G. Compton and C. E. Banks, *Understanding Voltammetry*, Imperial College Press, London, 2nd edn., 2011.
23 P. Chen and R. L. McCreery, *Anal. Chem.*, 1996, **68**, 3958–3965.
24 R. L. McCreery, *Chem. Rev.*, 2008, **108**, 2646–2687.
25 D. J. Martin, B. D. McCarthy, N. A. Piro and J. L. Dempsey, *Polyhedron*, 2016, **114**, 200–204.
26 D. J. Martin, B. D. McCarthy, C. L. Donley and J. L. Dempsey, *Chem. Commun.*, 2015, **51**, 5290–5293.
27 C. Amatore, J. Pinson, J. M. Savéant and A. Thiebault, *J. Electroanal. Chem. Interfacial Electrochem.*, 1980, **107**, 59–74.
28 B. D. McCarthy, C. L. Donley and J. L. Dempsey, *Chem. Sci.*, 2015, **6**, 2827–2834.
29 E. Anxolabéhère-Mallart, C. Costentin, M. Fournier and M. Robert, *J. Phys. Chem. C*, 2014, **118**, 13377–13381.
30 E. Anxolabéhère-Mallart, C. Costentin, M. Fournier, S. Nowak, M. Robert and J.-M. Savéant, *J. Am. Chem. Soc.*, 2012, **134**, 6104–6107.
31 S. El Ghachtouli, M. Fournier, S. Cherdo, R. Guillot, M.-F. Charlot, E. Anxolabéhère-Mallart, M. Robert and A. Aukauloo, *J. Phys. Chem. C*, 2013, **117**, 17073–17077.
32 K. J. Lee, N. Elgrishi, B. Kandemir and J. L. Dempsey, *Nat.*

Rev. Chem., 2017, **1**, 0039.
33 D. J. Sconyers and J. D. Blakemore, *Chem. Commun.*, 2017, **53**, 7286–7289.
34 R. H. Crabtree, *Chem. Rev.*, 2015, **115**, 127–150.
35 S. M. Barnett, K. I. Goldberg and J. M. Mayer, *Nat. Chem.*, 2012, **4**, 498–502.
36 Y. Surendranath, D. A. Lutterman, Y. Liu and D. G. Nocera, *J. Am. Chem. Soc.*, 2012, **134**, 6326–6336.
37 M. Fang, M. H. Engelhard, Z. Zhu, M. L. Helm and J. A. S. Roberts, *ACS Catal.*, 2014, **4**, 90–98.
38 A. J. Bard and L. R. Faulkner, *Electrochemical Methods: Fundamentals and Applications*, John Wiley & Sons, Inc., Hoboken, NJ, USA, 2nd edn., 2001.
39 N. D. Schley, J. D. Blakemore, N. K. Subbaiyan, C. D. Incarvito, F. D'Souza, R. H. Crabtree and G. W. Brudvig, *J. Am. Chem. Soc.*, 2011, **133**, 10473–10481.
40 L. Chen, G. Chen, C. Leung, S. Yiu, C. Ko, E. Anxolabéhère-Mallart, M. Robert and T.-C. Lau, *ACS Catal.*, 2015, **5**, 356–364.
41 B. J. Palys, G. J. Puppels, D. van den Ham and D. Feil, *J. Electroanal. Chem.*, 1992, **326**, 105–112.
42 K. Koshiba, K. Yamauchi and K. Sakai, *Angew. Chemie Int. Ed.*, 2017, **56**, 4247–4251.
43 A. Galtayries and J. Grimblot, *J. Electron Spectros. Relat. Phenomena*, 1999, **98–99**, 267–275.
44 D. A. Buttry and M. D. Ward, *Chem. Rev.*, 1992, **92**, 1355–1379.
45 G. Sauerbrey, *Zeitschrift für Phys.*, 1959, **155**, 206–222.
46 J. L. Dempsey, J. R. Winkler and H. B. Gray, in *Comprehensive Inorganic Chemistry II*, eds. J. Reedijk and K. Poeppelmeier, Elsevier, Oxford, 2013, vol. 8, pp. 553–565.
47 O. Pantani, S. Naskar, R. Guillot, P. Millet, E. Anxolabéhère-Mallart and A. Aukauloo, *Angew. Chemie Int. Ed.*, 2008, **47**, 9948–9950.
48 B. Lassalle-Kaiser, A. Zitolo, E. Fonda, M. Robert and E. Anxolabéhère-Mallart, *ACS Energy Lett.*, 2017, **2**, 2545–2551.
49 S. Cherdo, S. El Ghachtouli, M. Sircoglou, F. Brisset, M. Orio and A. Aukauloo, *Chem. Commun. (Camb).*, 2014, **50**, 13514–6.
50 C. Amatore, J. Pinson, J.-M. Savéant and A. Thiebault, *J. Electroanal. Chem. Interfacial Electrochem.*, 1979, **107**, 59–74.
51 A. Houmam, E. M. Hamed and I. W. J. Still, *J. Am. Chem. Soc.*, 2003, **125**, 7258–7265.
52 C. C. L. McCrory, C. Uyeda and J. C. Peters, *J. Am. Chem. Soc.*, 2012, **134**, 3164–3170.
53 E. S. Andreiadis, P.-A. Jacques, P. D. Tran, A. Leyris, M. Chavarot-Kerlidou, B. Jousselme, M. Matheron, J. Pécaut, S. Palacin, M. Fontecave and V. Artero, *Nat. Chem.*, 2013, **5**, 48–53.
54 W. R. McNamara, Z. Han, P. J. Alperin, W. W. Brennessel, P. L. Holland and R. Eisenberg, *J. Am. Chem. Soc.*, 2011, **133**, 15368–15371.

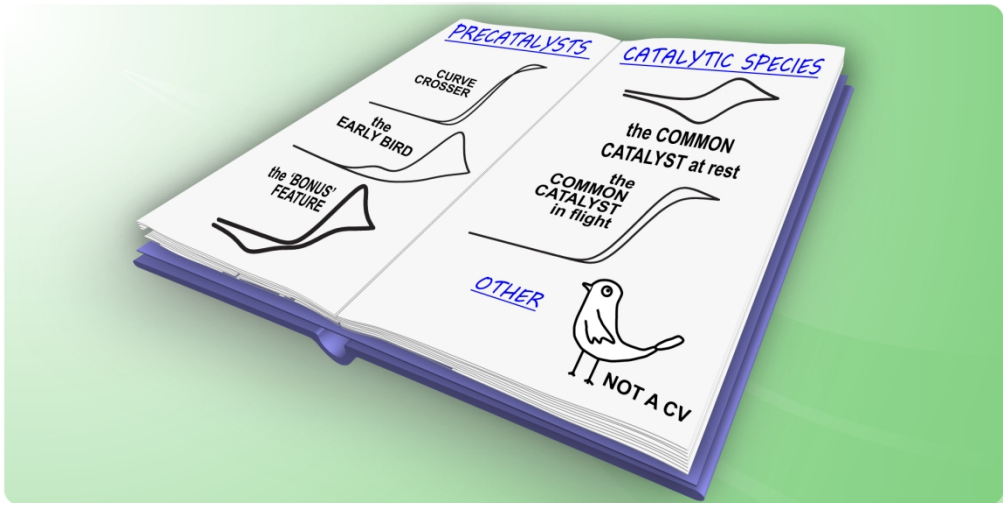
PRECATALYSTS
CURVE CROSSER
the EARLY BIRD
the 'BONUS' FEATURE
CATALYTIC SPECIES
the COMMON CATALYST at rest
the COMMON CATALYST in flight
OTHER
NOT A CV